ON EDDY DIFFUSION PROFILES IN OCEANIC BOTTOM BOUNDARY LAYERS ASSOCIATED WITH COLD EDDIES AND FILAMENTS

TAL EZER[1] and GEORGES L. WEATHERLY[1,2]

[1]*Department of Oceanography, Florida State University, Tallahassee, FL 32306-3048*
[2]*Geophysical Fluid Dynamics Institute, Florida State University, Tallahassee, FL 32306*

(Received in final form 23 December, 1988)

Abstract. The oceanic bottom boundary-layer model of Weatherly and Martin (1978) is used to study the vertical structure of the eddy diffusivity in a region with initially imposed bottom mixed-layer thickness. Because of near-bottom oceanic features, such as the Cold Filament (Weatherly and Kelley, 1982) and cold eddies (Ebbesmeyer *et al.*, 1988), the bottom mixed-layer thickness is not the sole result of boundary-layer mixing; this is the incentive for this study. For a given geostrophic forcing and imposed mixed-layer depth, a formula for the eddy diffusion coefficient is found. This parameterization of the eddy diffusivity improves previous formulas used in oceanic and atmospheric boundary layers in the upper portion of the boundary layer. A simple model of a Cold Filament-like feature demonstrates the structure of the bottom boundary layer, the bottom mixed layer, and the relation between the two. A lens-like cross section of cold blobs, often used in analytical models, may be inappropriate if bottom friction is important.

Preface

Since this is a study of the oceanic bottom boundary layer, some explanation is in order as to why it was submitted to this journal. Many oceanographers interested in boundary-layer processes read *Boundary-Layer Meteorology*. However, we think that this study may also be of interest to some atmospheric boundary-layer researchers. For example, it may be of direct relevance to meteorologists interested in parameterizing vertical diffusivity profiles in nocturnal atmospheric boundary layers or in atmospheric boundary layers in polar regions. In any event, we are grateful to the editor and the reviewer for allowing us to publish a paper on the **other** boundary layer of this planet in *Boundary-Layer Meteorology*.

1. Introduction

Measurements in the ocean indicate a layer above its bottom tens of meters thick that is well-mixed and homogeneous in potential temperature and salinity (hence density), and suspended sediment (e.g., Figure 1). Amos *et al.* (1971), who first documented the existence of these bottom mixed layers in the deep ocean, offered two explanations. "(1) A homogeneous water mass is flowing beneath another water mass for considerable distance, and intermixing of these two masses is restricted by the stable layer which forms their vertical boundary and (2) A turbulent boundary-layer thickness exists at the bottom causing a mixed

Boundary-Layer Meteorology **48**: 83–97, 1989.

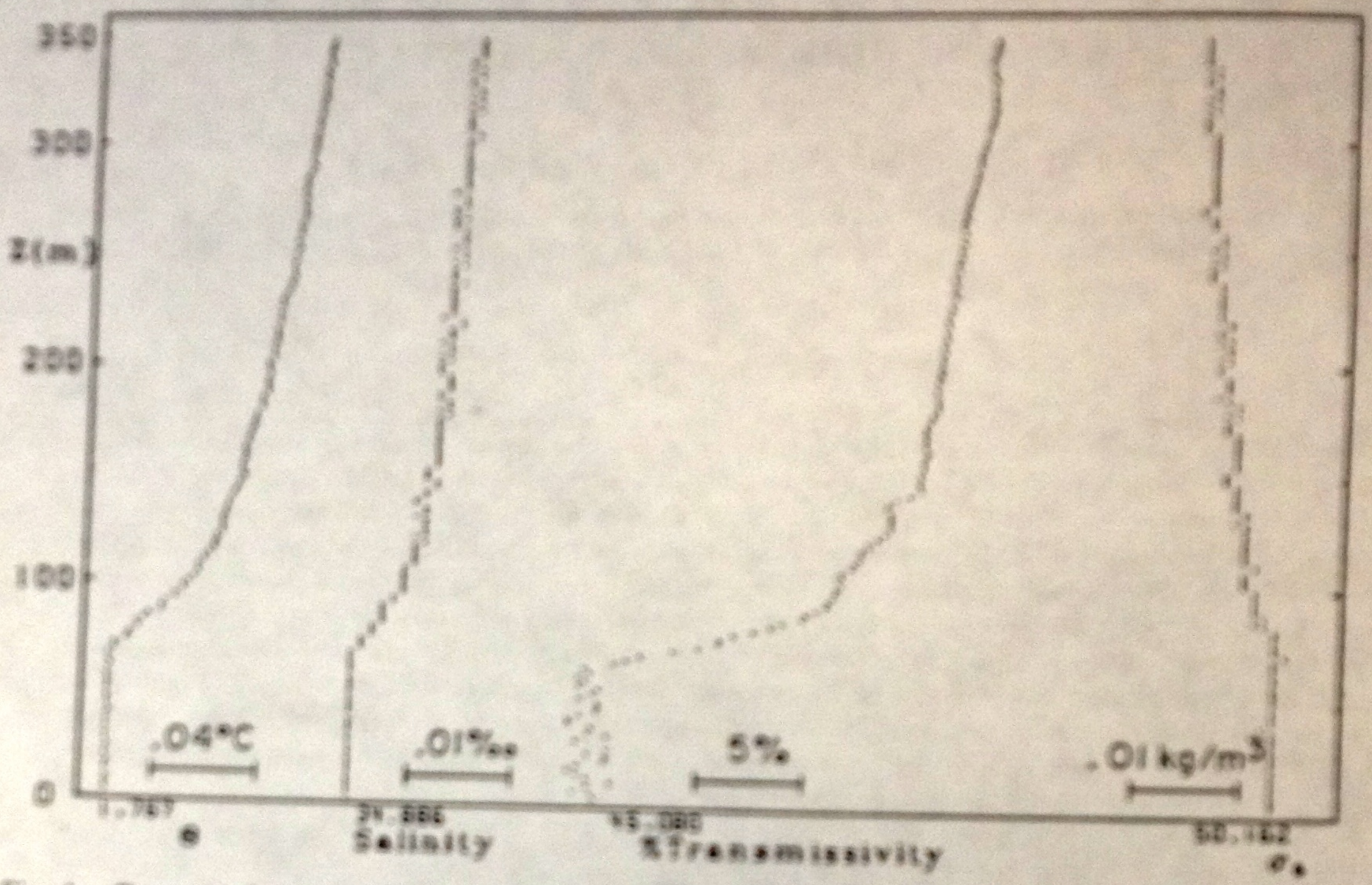

Fig. 1. Example, from Weatherly and Kelley (1982), of a deep ocean bottom mixed layer, in this case from the *Cold Filament* (see text). Going from left to right, profiles of: potential temperature, salinity, optical transmissivity of 660 nm light over a 1 m path length [(1-transmissivity) is an index of the suspended bottom sediment concentration], and potential density referenced to 500 atmospheres pressure (the pressure at about 5000 m depth where the observations were made).

(homogeneous) layer whose thickness is dependent upon the roughness of the bottom . . . and the magnitude of the current." Weatherly and Kelley (1982) noted that both types of oceanic bottom mixed layers (hereafter denoted by BML's) are common in the deep ocean. This study is concerned with oceanic bottom boundary layers formed in BML's of the first type.

At the onset, it should be noted that unlike the atmospheric boundary layer, the heat flux across the bottom is unimportant generally for the oceanic bottom boundary layer (hereafter denoted by BBL). First, it has long been recognized (e.g., Wimbush and Munk, 1970) that the geothermal heat flux has a neglible effect (i.e., the Monin–Obukhov length scale associated with the geothermal heat flux ≫ the BBL thickness). However, a second heat flux across the bottom is relevant to the present study. The BML's considered here are associated (as discussed further below) with anomalously cold bottom water masses. These layers do migrate over the ocean floor, and because of this, they may be at times of order 0.1 °C colder than the ocean bottom. Adams (personal communication, 1988) studied the thermal interaction of ocean bottom sediments and the overly-

ing BBL for initial temperature difference between them of order ± 1 °C. He found that the resulting heat flux at the bottom had a negligible effect on the dynamics and structure of the BBL. The model used by Adams is an expanded version of the one discussed in Adams and Weatherly (1981). We therefore conclude that for the present study, heat flux across the ocean floor has a negligible effect on the turbulence in the BBL.

Studies at the base of the Scotian Rise (~40° N 60° W), water depth 5000 m, indicate that the BBL is much thicker than the one expected from conventional scaling with comparable velocity and stratification. In this area, a bottom mixed layer of thickness 20–100 m and an overlying transition layer which extends up to ~200 m above the ocean bottom coincide with the structure of the Cold Filament (Weatherly and Kelley, 1982; 1985). Characteristic properties of this region are geostrophic velocity $V_g = 0.15\,\mathrm{m\,s^{-1}}$, Brunt-Vaisala frequency above the BML $N = 10^{-3}\,\mathrm{s^{-1}}$, and Coriolis parameter $f = 10^{-4}\,\mathrm{s^{-1}}$. If the friction velocity is estimated by $u_* = 0.03\,V_g$, the thickness of the bottom boundary layer h approximated by

$$h = (1.3u_*/f)[1 + (N/f)^2]^{-1/6} \tag{1}$$

(Weatherly and Martin, 1978) is only ~18 m. Note that for values of N representative of the deep ocean, (1) reduces to the familiar

$$h = 0.4(u_*/f)\,. \tag{2}$$

Diffusion of turbulent kinetic energy, which is not included in the derivation of (1), enables the boundary-layer thickness to reach larger values than the above approximation (Richards, 1982), but still not comparable to the observed scales. Equation (1) is the boundary-layer thickness formed in an initially stably stratified ocean with constant N. In such a case, the bottom mixed layer is coincident with the bottom boundary layer defined to be the height where the turbulent kinetic energy vanishes (Weatherly and Martin, 1978). (This is essentially the second type of BML proposed by Amos *et al.*). However, the potential temperature profiles inside the Cold Filament (CF) as well as elsewhere in the western North Atlantic (e.g., Ebbesmeyer *et al.*, 1986; Weatherly and Kelley, 1982, 1985), indicate BML's too cold for such a formation. Therefore, we must take into account the imposed scale of the CF height (which is the coupled result of the dynamics of the CF and BBL formation), and consider a more general case in which the BML is not necessarily the same as the BBL. Another argument to support such an approach is that the boundary layer has a "memory" of previous mixings, and thus initial stratification of a mixed layer may be more appropriate than that of a constant density gradient. To emphasize that the BML thickness may be different from that of the BBL, we shall denote the former by H, and the latter by h.

In the first part of this study, the one-dimensional model of Weatherly and Martin (1978), which is based on Mellor and Yamada (1974) level II turbulence

closure scheme with minor modifications, is used to calculate vertical profiles of the eddy diffusion coefficient for momentum $K(z)$. Under the conditions discussed here, the K profiles calculated by this model are very similar to those given by the more complicated level $II\frac{1}{2}$ models. For a given geostrophic velocity and imposed initial stratification with BML thickness H, an empirical formula for $K(z)$ is suggested. In the second part, a simple two-dimensional model of the Cold Filament is presented to examine the structure of the BBL and the BML.

2. Parameterization of the Eddy Diffusivity

Taking initial potential temperature profiles with different mixed-layer depths as those reported by Weatherly and Kelley (1982), and constant geostrophic forcing, a steady state is reached by the model within a time scale of a few days. The final temperature profiles are similar to the initial ones, provided the initial mixed layer is equal to or greater than h given by Equation (1). Otherwise the final mixed layer is thicker than the initial one but consistent with (1). The calculations were done for the following range of parameters: initial mixed-layer thickness $30\,\mathrm{m} < H < 110\,\mathrm{m}$, geostrophic velocity $0.05\,\mathrm{m\,s^{-1}} < V_g < 0.25\,\mathrm{m\,s^{-1}}$, and roughness length $0.01 \times 10^{-2}\,\mathrm{m} < z_0 < 1 \times 10^{-2}\,\mathrm{m}$, which covers most of the expected values in benthic boundary layers. Since the model is fairly insensitive to the choice of z_0, a value of $z_0 = 0.016 \times 10^{-2}\,\mathrm{m}$ was used unless otherwise indicated. This value is the average roughness parameter for this region (Gross *et al.*, 1986). For this value of z_0, the friction velocity $u_* \approx 0.035\ V_g$, but for larger values, u_* may better be estimated by relations of the form

$$V_g/u_* = F[\ln(R_0)]\,, \tag{3}$$

where F is a function of the frictional Rossby number $R_0 = u_*/(fz_0)$ (e.g., Tennekes and Lumley, 1972).

The profiles of the eddy diffusion coefficient calculated for the different velocities and temperature profiles show the following characteristics:

(a) In cases where the imposed mixed-layer thickness H is larger than $\sim 1.3(u_*/f)$, the eddy diffusion coefficient profile is identical to that of a neutrally stratified case as expected from the fact that the turbulent kinetic energy vanishes at height $\sim 1.3(u_*/f)$ [i.e., Equation (1) with $N = 0$].

(b) In cases where $H \leq 1.3(u_*/f)$, the eddy diffusion coefficient vanishes at the base of the transition region (Figure 2a–2d), i.e., the BBL occupies all of the BML.

(c) Both K_{max} and z_{max}, the maximum K and the level where it occurs, increase slightly with increasing H, but the ratio between K_{max} and $u_* z_{max}$ is independent of H (Figure 3a) and can be written as

$$K_{max} = (k u_* z_{max}) e^{-1}\,, \tag{4}$$

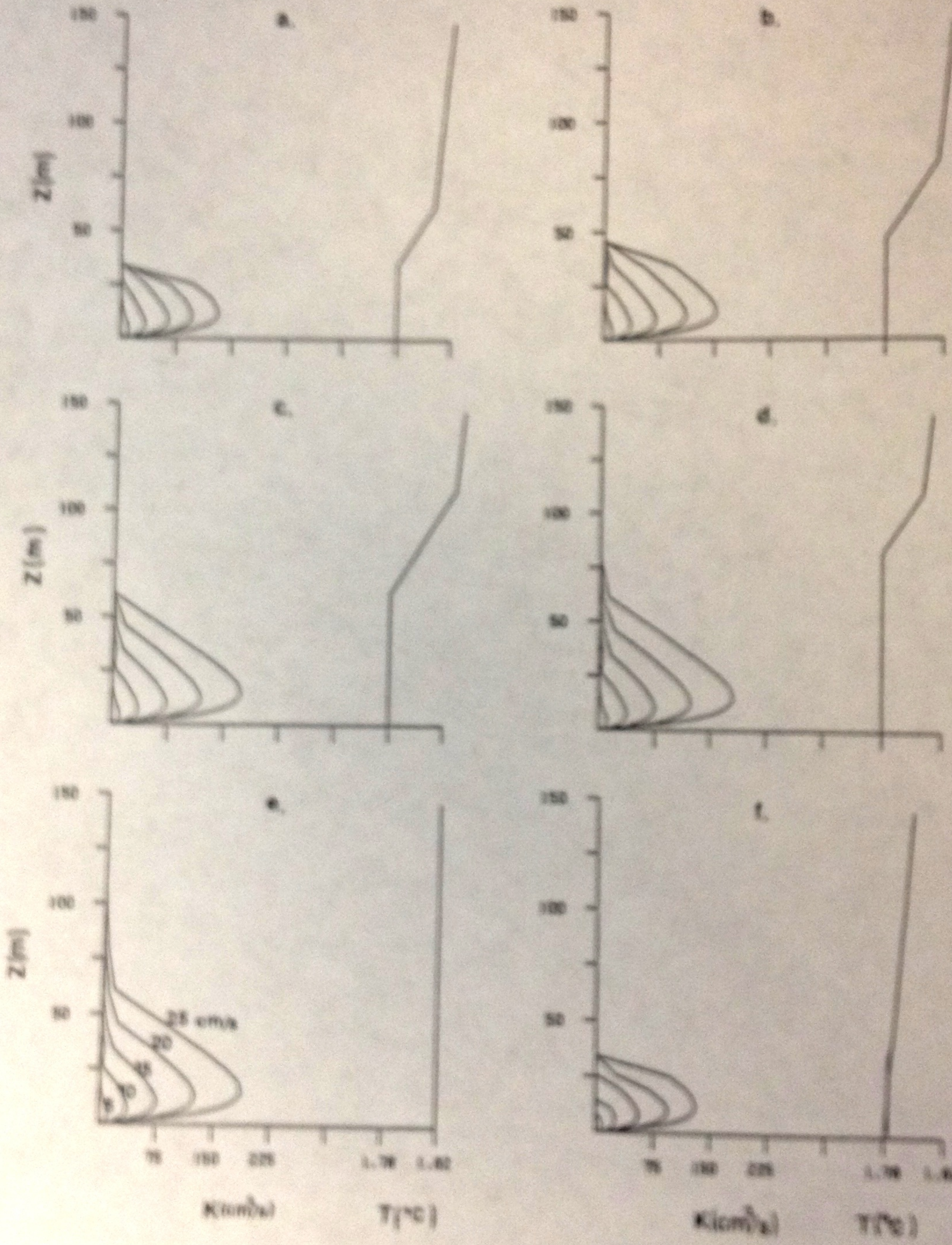

Fig. 2. Initial potential temperature profiles (right), and eddy diffusion coefficient profiles (left), calculated by the numerical model for geostrophic velocities $V_g = 0.05, 0.1, 0.15, 0.2$, and $0.25\ m\ s^{-1}$, and imposed BML thickness H: (a) $H = 34$ m; (b) $H = 46$ m; (c) $H = 61$ m; (d) $H = 82$ m. In (a) the stratification is neutral everywhere, and in (f) the stratification is initially uniform. The final stratification is identical to the initial one for (a)–(e), and for (f) it is shown for $V_g = 0.25\ m\ s^{-1}$. The same temperature gradient (i.e., N) across the transition region is taken in Figure (a)–(e).

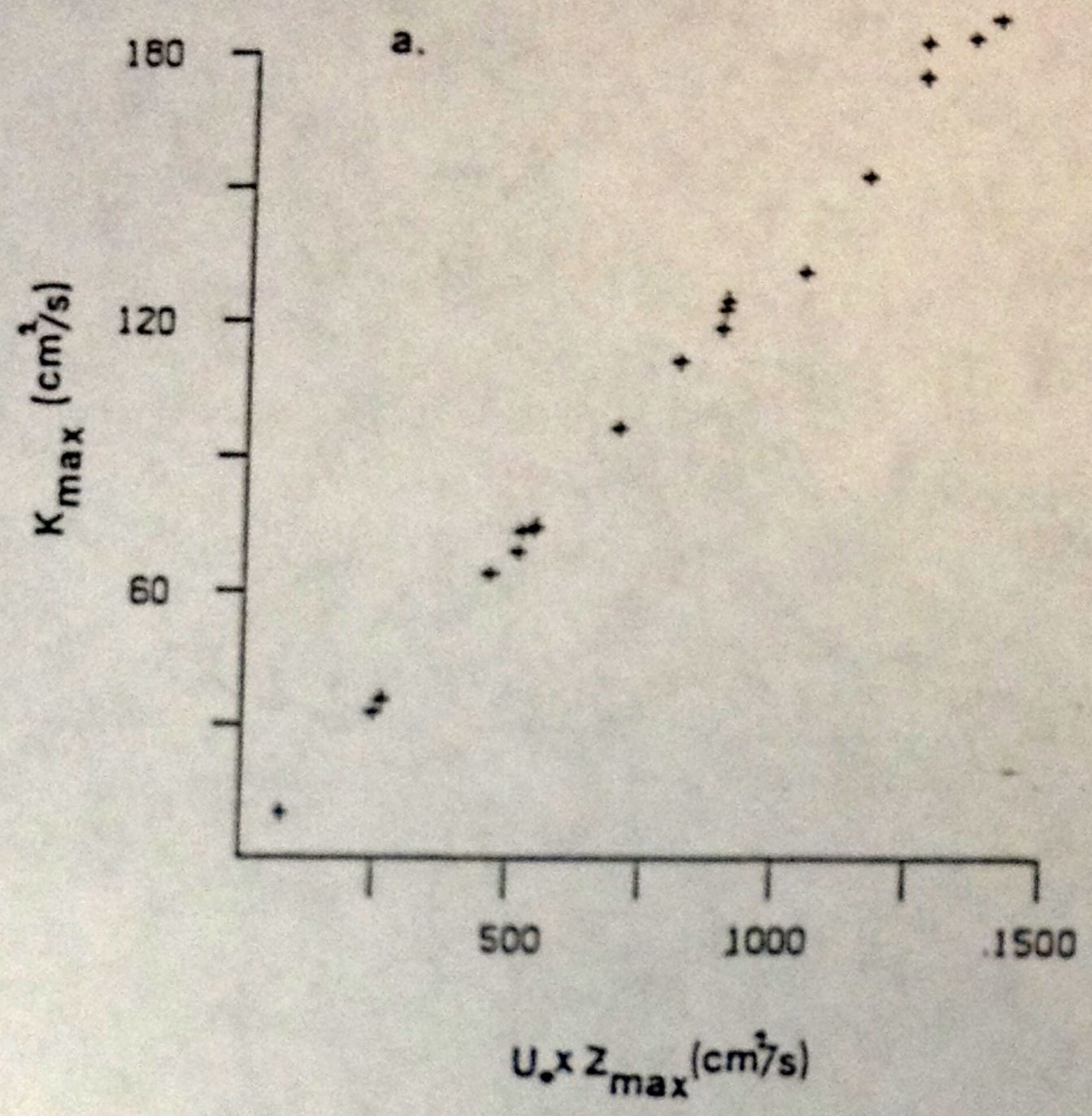

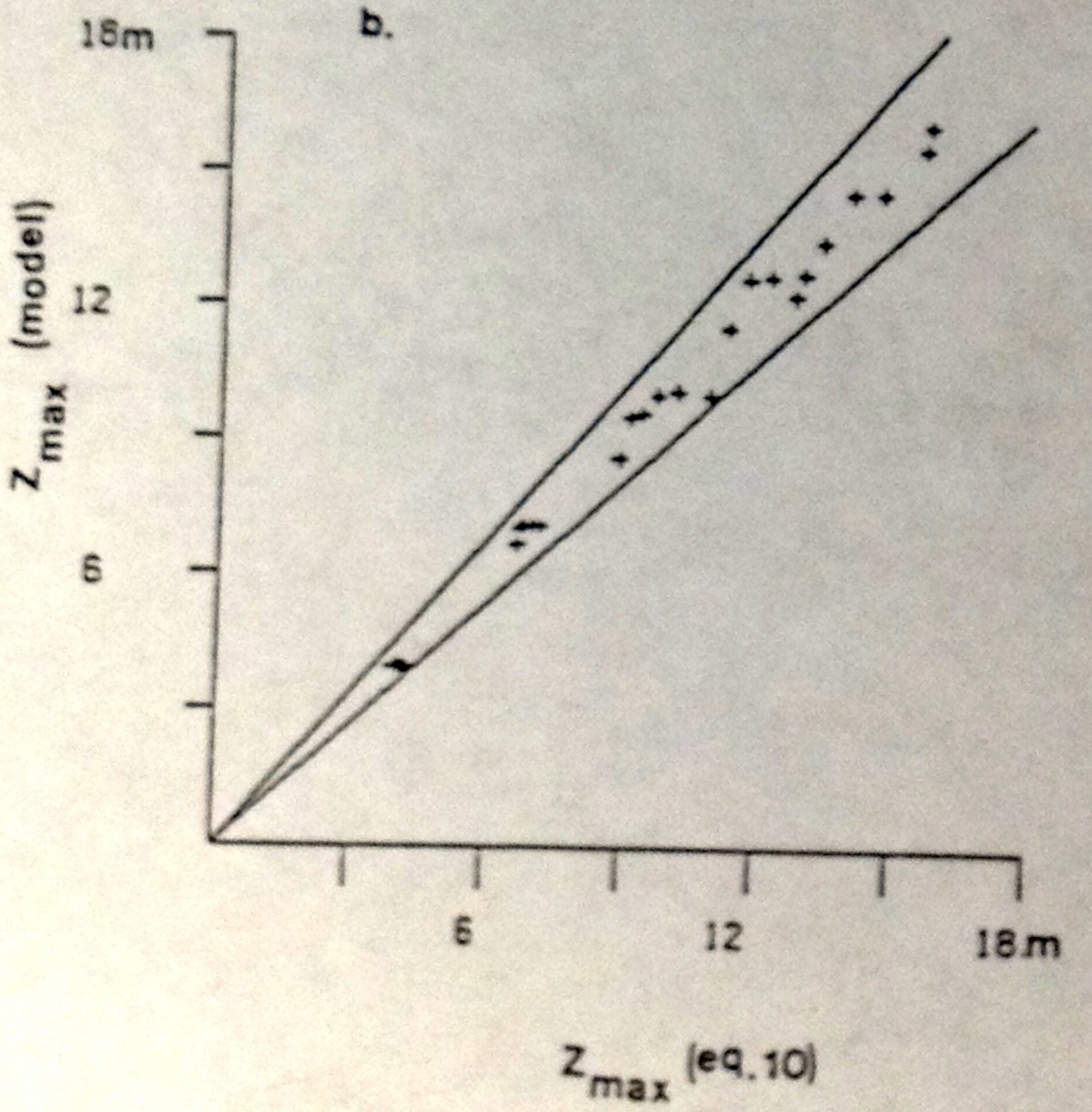

Fig. 3. (a) The distribution of K_{max} vs. $u_* z_{max}$, calculated by the model for $V_s = 0.05, 0.1, 0.15, 0.2$, and $0.25\ m\ s^{-1}$, and for $H = 34, 46, 61, 82, 109$ m, and neutrally stratified case. (b) Z_{max} calculated by the model vs. Z_{max} calculated by (10) for all the cases of Figure 2a. The range between the two lines represents the uncertainty in the values calculated by the model due to the model's resolution.

where $k = 0.4$ is von Karman's constant. A similar relation was suggested by Wippermann (1974).

(d) A major effect of the imposed scale is to change the shape of the K profile in the upper part of the mixed layer.

A comparison with the BML formed from constant density gradient (Figure 2f) shows that this kind of BML formation results in unrealistic temperature profiles for the Cold Filament and too thin a BBL while the imposed mixed-layer method agrees with the observations (e.g., Weatherly and Kelley, 1982, 1985). The basic difference between the two approaches is that in the formation of BBL from an initially constant potential density gradient profile, the development of eddy kinetic energy is limited by the initial potential energy of the stable stratification, while a specified non-zero BML thickness enables the BBL to be developed in neutral stratification with a much larger length scale.

Many models of boundary layers based on different assumptions and different closure schemes produce fairly similar eddy diffusion profiles (e.g., Lettau and Dabberdt, 1970; Businger and Arya, 1974; Wyngaard *et al.*, 1974; Wippermann, 1974; Weatherly, 1975; Weatherly and Martin, 1978, Richards, 1982). Thus it is tempting to specify the eddy diffusion coefficient in a simple formula. Parameterizations of different forms (but again with fairly similar structure) can be found in O'Brien (1970), Lettau and Dabberdt (1970), Businger and Arya (1974), Wippermann (1974), Brost and Wyngaard (1978), and Gryning *et al.* (1983). However, none of the above uses an imposed mixed-layer depth much different than the one estimated by simple diagnostic relations such as (1) or (2). Arya (1973) compared different K-models and showed that eddy diffusion coefficient structure of the form

$$K(z) = azu_* e^{-z/b}\,, \tag{5}$$

with a and b constants, gives a wind shear profile which is in good agreement with the Deardorff (1970) model. The relation (4) can be recovered from (5) by letting $a = k$ and $b = z_{\max}$. The exponential K profile of (5) agrees quite well with our model calculations in the lower portion of the BML but gives a poor description of the K profile in the upper portion. As indicated by Businger and Arya (1974), the assumptions that led to the derivation of (5) are not valid in the upper part of the boundary layer.

Therefore, we try to find an expression for $K(z)$ which is realistic both in the lower and upper portions. A formula of the form

$$K(z) = ku_* z(a_0 + a_1 z + a_2 z^2 + \cdots) e^{-z/z_{\max}}\,, \tag{6}$$

where a_i may be some functions of H and $z_{\max}$, is sought. We require (6) to satisfy the following conditions: $K = 0$ at $z = 0,\ H$; K reaches its maxima at $z = z_{\max}$; (6) satisfies (4). At least three terms are then needed, and the coefficients are found to be

$$[a_0, a_1, a_2] = (H - z_{\max})^{-2}[(H^2 - 2z_{\max}H), 2z_{\max}, -1]\,. \tag{7}$$

Another requirement that these coefficients must satisfy is that $a_0/a_1 >$ the logarithmic layer thickness (say, $0.15H$) so that in the logarithmic layer, K is linear with z (the third term can be neglected for small z). This ratio is given by

$$a_0/a_1 = H(H/2z_{max} - 1)\,, \tag{8}$$

and implies a restriction on the length scale z_{max}, namely that $z_{max} < 0.43H$. For all the results presented here, this condition is satisfied. Now, (6) can be written as

$$K(z) = ku_* z\left[1 - \frac{(z - z_{max})^2}{(H - z_{max})^2}\right] \exp\left[\frac{-z}{z_{max}}\right], \quad 0 < z < H\,. \tag{9}$$

For $z > H$, K can be chosen as the molecular viscosity or a small value representing the turbulence in the interior.

However, the problem is not closed until z_{max} is specified in terms of the known parameters V_g and H. Following Businger and Arya (1974), the non-dimensional ratio $z_{max}/(u_*/f)$ is scaled like the ratio u_*/V_g. Thus z_{max} should be proportional to the length scale $l_0 = u_*^2/(V_g f)$. We take

$$z_{max} = 1.7[l_0(2 + H/h_{max}) + l_1(1 - H/h_{max})]\,, \tag{10}$$

where $l_1 = 1$ m and $h_{max} = 1.3(u_*/f)$ are an empirical length scale and the BBL thickness in neutral stratification, respectively. A comparison of (10) to the z_{max} calculated by model (Figure 3b) shows good agreement within the range of uncertainty due to the variable model grid (the model has finer resolution near

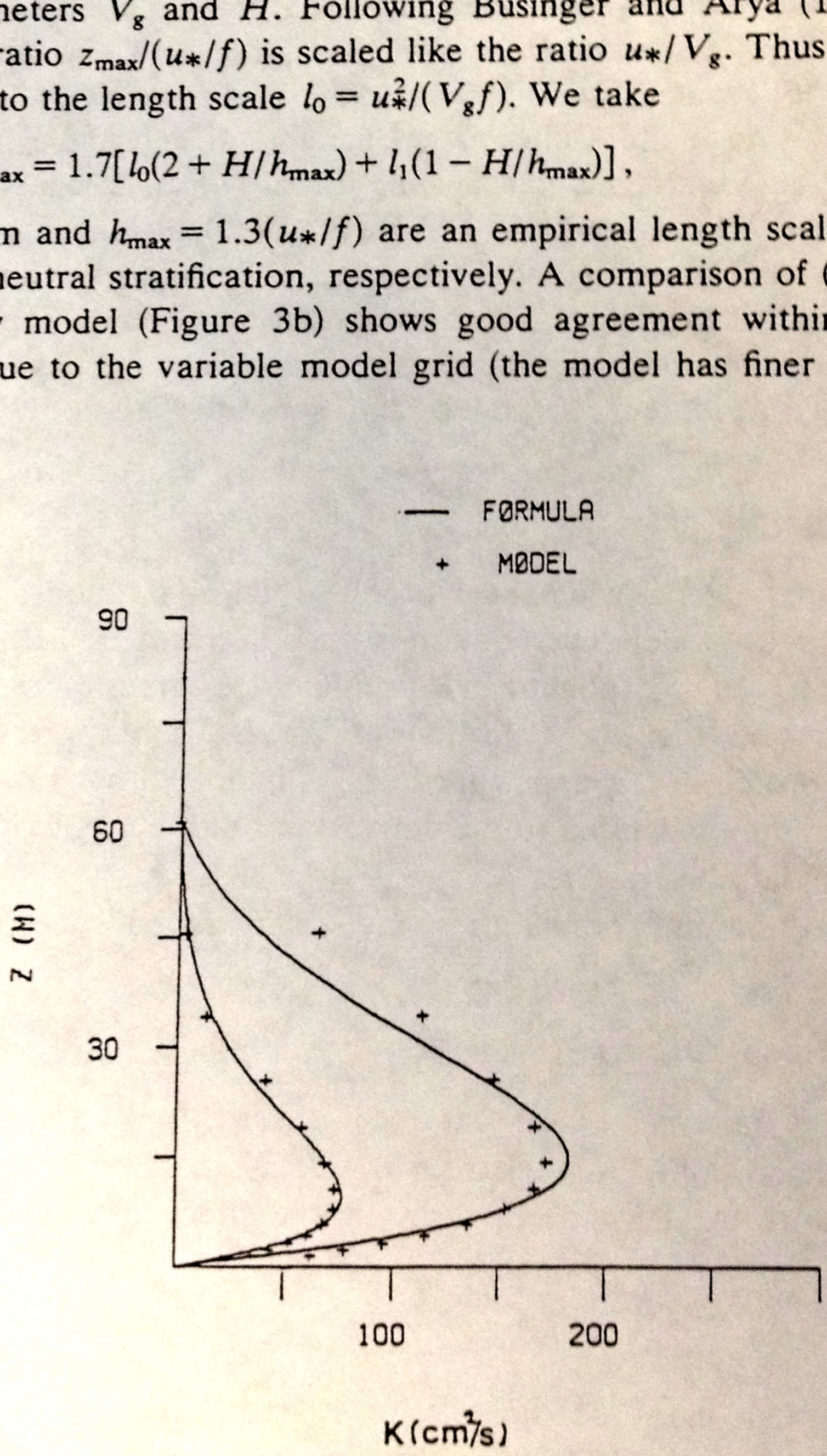

Fig. 4. A comparison between the structure of the eddy diffusion coefficient calculated by (9) (solid lines), and that calculated by the numerical model ("+"), for $H = 61$ m and $V_g = 0.15$ and 0.25 m s^{-1}.

the bottom). For the neutrally stratified case, (10) reduces to $z_{max} \approx 0.16(u_*/f)$, which is the value suggested by Long (1981) and Mofjeld and Lavelle (1984).

Now, for given values of geostrophic velocity V_g and imposed mixed-layer scale H, the friction velocity can be found by (3), the height of maximum eddy viscosity z_{max} can be found by (10) and the vertical profile of the eddy diffusion coefficient $K(z)$ is specified by (9). The general structure of the eddy diffusion coefficient given by (9) is in good agreement with the model (e.g., Figure 4). The discrepancy between the formula and the model decreases as V_g decreases.

All the above formulations were found for the cases where the BML thickness $H \geq h$, where h is the BBL thickness given by (1). For $H < h$, the BML thickened, as noted earlier, until its thickness was in agreement with (1). Therefore, we conclude that our formulas are valid for $H \geq 1.3(u_*/f)[1 + N^2/f^2]^{-1/4}$ with N being a representative value for the lower transition region above the BML.

3. The Spatial Structure of the Bottom Boundary Layer in the Cold Filament (CF)

In this section, the findings of the previous section are applied to a Cold Filament (CF)-like feature, in order to study the structure of the BBL and the BML and the relations between the two.

We take a two-dimensional (i.e., no variations in the y-direction) homogeneous filament (representing the CF core) of dense water, embedded in a stationary stratified interior, on a sloping bottom. The downslope is in the x-direction, and the inclination angle α is small (i.e., $\tan(\alpha) \approx \alpha$) so the bottom is defined by $z_B = -\alpha x$. For the CF, $\alpha \approx 0.005$. The initial CF core thickness is specified as

$$H_I(x) = H_0[1 - (x/x_0)^2], \tag{11}$$

which is in a similar form to the cross-section of a cold eddy with a linear orbital velocity profile (Nof, 1984). The maximum thickness of the core is taken as $H_0 = 100$ m (Weatherly and Kelley, 1982), and the radius is taken as $x_0 = 5$ km (Ezer and Weatherly, 1988). The density field is assumed to result solely from the potential temperature field with a linear equation of state,

$$\rho = \rho_0[1 - \beta(\theta - \theta_0)], \tag{12}$$

where $\rho_0 = 1.028$ gr cm^{-3}, $\theta_0 = 1.78$ °C, and $\beta = 9.4 \times 10^{-5}$ °C^{-1}. β is chosen to give realistic values of N above the BML. The initial temperature field is taken as

$$\theta(x, z) = \begin{cases} \theta_0 & z \leqq H_I + z_B \\ \theta_1 - Bx \exp[(H_I + z_B - z)/z_1] & z > H_I + z_B, \end{cases} \tag{13}$$

where $\theta_1 = 1.83$ °C, $B = 0.05$, and $z_1 = 60$ m (e.g., Figure 5a). The coefficients in (12) and (13) are chosen to fit the temperature profiles measured by Weatherly and Kelley (1982) for the lower 200 m above the bottom.

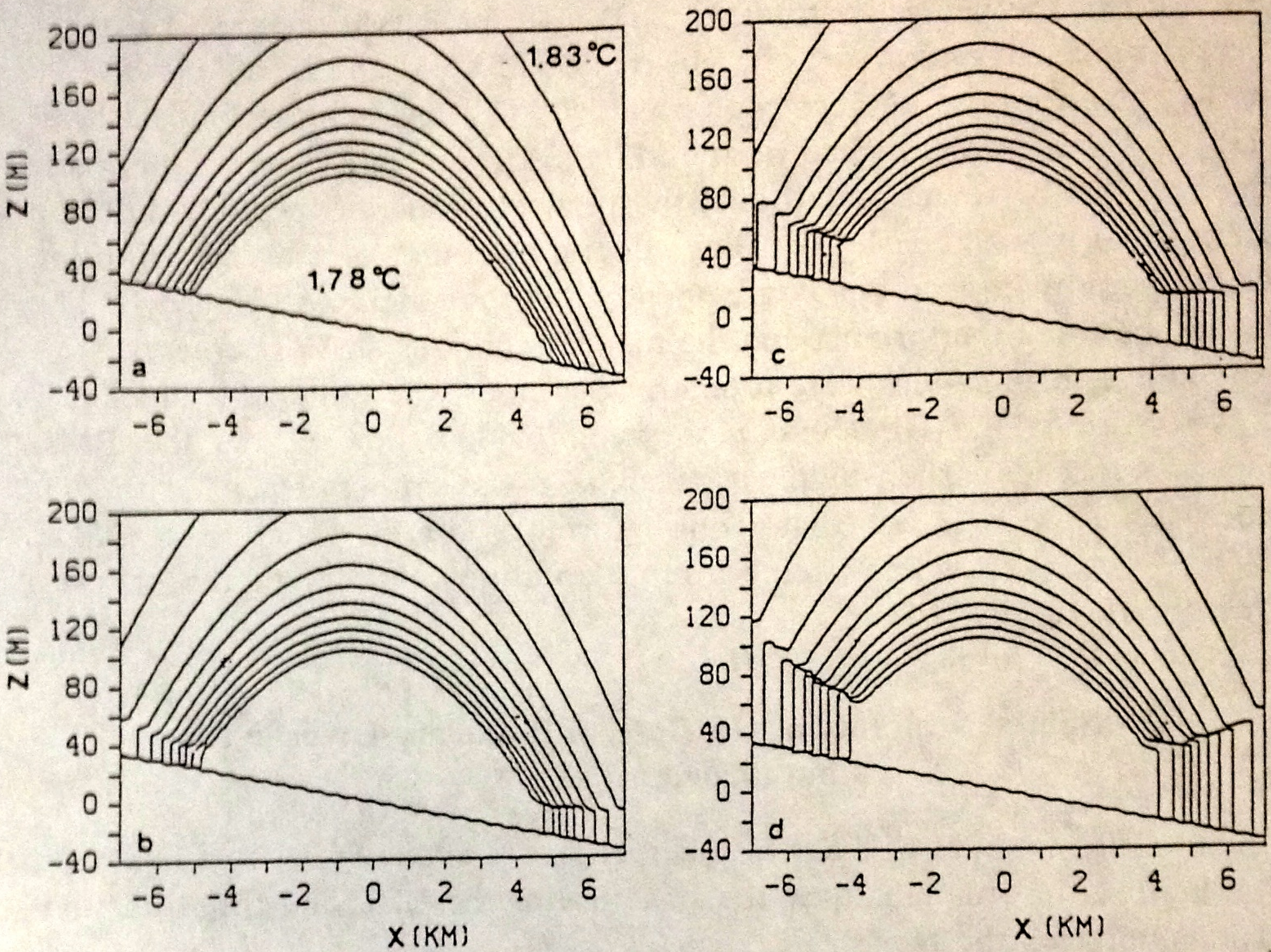

Fig. 5. The potential temperature structure calculated by the two-dimensional model of Section 3: (a) initial structure, (b), (c), and (d), are for $V_0 = -0.1$, -0.2, and $-0.3\ \mathrm{m\ s^{-1}}$, respectively.

Now, if the interior velocity at $z = H_T$ (well above the BML) is assumed to be constant, and $V_0 < 0$ (i.e., southward flow), using the hydrostatic approximation and (12), the geostrophic component can be estimated from the temperature field,

$$V_g(x, z) = V_0 - (\beta g/f) \int_z^{H_T} \theta_x \, \mathrm{d}z \,, \tag{14}$$

where g is the gravitational acceleration and the subscript x indicates partial derivative. Following Section 2, the thickness of the BBL and the BML are approximated by

$$h(x) = (1.3 u_*/f)[1 + (N/f)^2]^{-1/4} \tag{15a}$$

$$H(x) = \max[H_I, h] \,, \tag{15b}$$

where $N^2 = g\beta\theta_z$ and $u_* = 0.035|V_g|$ are taken according to the values on the top of the BBL. The calculations are done numerically with grid size of $\delta x = 250\ \mathrm{m}$ and $\delta z = 2.5\ \mathrm{m}$ in the region $-7\ \mathrm{km} < x < 7\ \mathrm{km}$ and $-40\ \mathrm{m} < z < 200\ \mathrm{m}$. The BML is calculated in the following way:

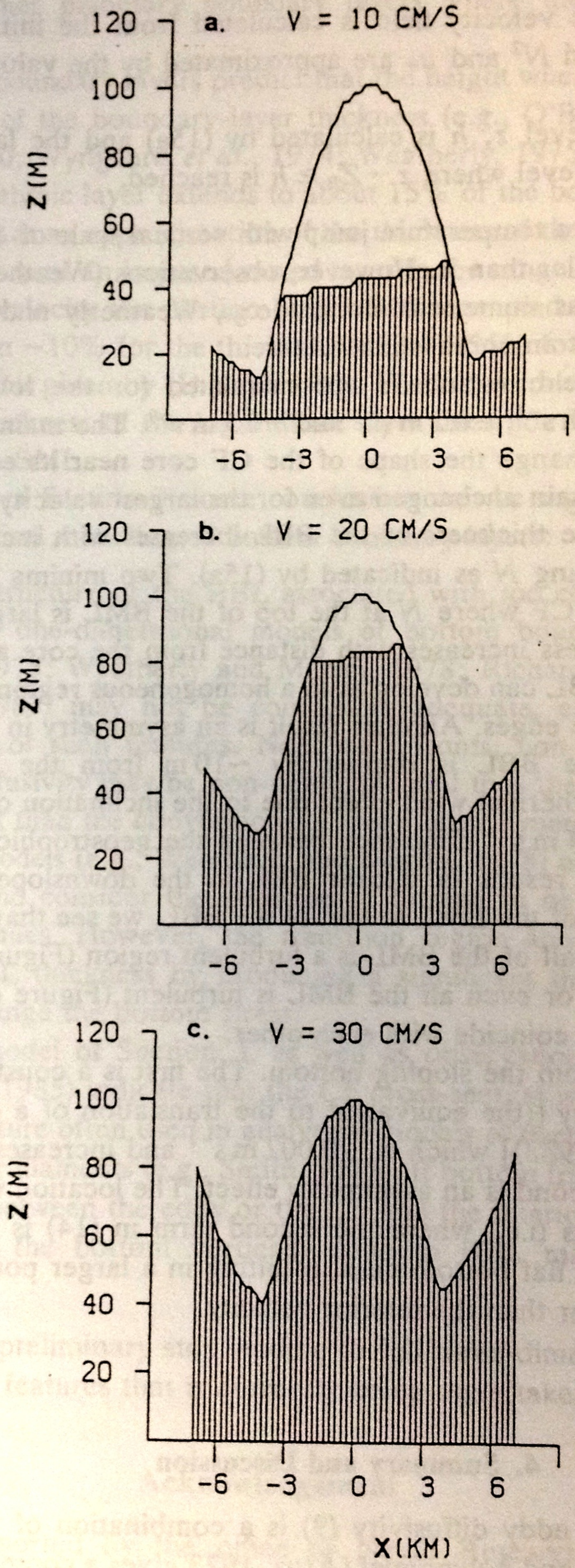

Fig. 6.– The thickness of the BML (outer line) and the thickness of the BBL (dashed area) for the velocities $V_0 = -0.1$, -0.2, and $-0.3\ \mathrm{m\ s^{-1}}$ as in Figure 4b, 4c, and 4d.

(1) The geostrophic velocity field is calculated from the initial temperature field by (14), and N^2 and u_* are approximated by the values of θ_z and V_g at each level.
(2) Then, at each level z, h is calculated by (15a) and the layers below are mixed until the level where $z - Z_B \geq h$ is reached.

This process produces a temperature jump with vertical scale of δz on top of the BML when H_t is smaller than h. However, observations (Weatherly and Kelley, 1982, 1985) as well as numerical models (e.g., Weatherly and Martin, 1978) indicate that this is not an unrealistic structure.

The temperature field, h and H are calculated for the following interior velocities: $V_0 = -0.1\,\mathrm{m\,s^{-1}}$, $-0.2\,\mathrm{m\,s^{-1}}$ and $-0.3\,\mathrm{m\,s^{-1}}$. The main effect of near-bottom mixing is to change the shape of the CF core near its edges; however, large portions of it remain unchanged even for the largest velocity examined here (Figures 5 and 6). The thickness of the BBL increases with increasing V_g but decreases with increasing N as indicated by (15a). Two minima of h are found near the edges of the CF where N at the top of the BML is large. Outside the core, the BML thickness increases with distance from the core as N decreases. Inside the core, the BBL can develop as in a homogeneous region creating sharp benthic fronts near the edges. Another result is an asymmetry in the BBL. Near the upslope edge, the BBL is thinner by ~10 m from the BBL near the downslope edge. The thermal wind effect due to the inclination of the transition region produces $\sim 0.04\,\mathrm{m\,s^{-1}}$ difference between the geostrophic component at the two edges, which results in thicker BBL in the downslope region. If we compare the structure of the BML to that of the BBL, we see that for velocity of $0.1\,\mathrm{m\,s^{-1}}$, only about half of the BML is a turbulent region (Figure 6a) while for larger velocities, most or even all the BML is turbulent (Figure 6b and 6c) and the BML and the BBL coincide with each other.

Two effects result from the sloping bottom. The first is a constant addition to the geostrophic velocity [(the equivalent to the translation of a cold eddy on a sloping bottom (Nof, 1983)] which is $\sim 0.002\,\mathrm{m\,s^{-1}}$ and increases somewhat the BBL thickness. The second is an asymmetry effect. The location where there are no thermal wind effects (i.e., where the second term in (14) is zero) is shifted upslope compared to a flat bottom case, resulting in a larger portion of the CF having velocities greater than the interior velocity.

4. Summary and Discussion

The expression for the eddy diffusivity (9) is a combination of two commonly used forms: exponential and polynomial (Arya, 1973 gives a comparison between the two). It is intended for oceanic applications where the BBL is formed in BML's thicker than expected due to local currents and stratifications. It should be

appropriate for other planetary boundary layers where the BML is initially specified.

Many studies of boundary layers predict that the height where K is a maximum is about one third of the boundary-layer thickness (e.g., O'Brien, 1970; Lettau and Dabberdt, 1970; Wyngaard *et al.*, 1974; Weatherly, 1975). If, as commonly assumed, the logarithmic layer extends to about 15% of the boundary layer, then $z_{max}/2$ can be taken as an approximation of the thickness of the logarithmic layer. However, for the case of an imposed mixed layer in the range discussed here, for every geostrophic velocity the portion of the BBL occupied by the logarithmic layer varies between ~10% for the thickest BML to ~25% for the thinnest BML (where the lower limit given by (1) is reached). The latter conclusion results from the fact that the thickness of the logarithmic layer does not depend strongly on the thickness of the BML.

From the results of Section 3, some conclusions can be suggested for further analytical or numerical modeling of bottom boundary layers:

(a) The spatial structure of the BBL associated with too cold benthic layers, suggests that one-dimensional models of bottom boundary layers (e.g., Weatherly, 1975; Weatherly and Martin, 1978; Richards, 1982; McLean and Yean, 1987) may not be completely adequate, especially near the lateral edges of such features. Near such fronts, non-linear effects and horizontal diffusivity may be non-negligible and thus the dynamics may be quite different than the conventional Ekman layer dynamics.

(b) Some BBL models (e.g., Weatherly and Martin, 1978) neglect the thermal wind effect and consider the geostrophic forcing to be solely due to the interior dynamics. However, the transition region above the BML may affect the BBL thickness by producing a significant thermal wind effect which can change the bottom stress.

(c) The simple model of Section 3, as well as observations (Weatherly and Kelley, 1982, 1985) indicate that the CF cross-section is different than the lens-like structure often used in analytical models of deep eddies (e.g., Nof, 1983, 1984) or filaments (e.g., Smith, 1975). If bottom friction is important, the interface between the eddy or the CF and the interior is more likely to intersect with the bottom vertically (due to BBL mixing) rather than obliquely.

This study is only a preliminary step leading to full three-dimensional numerical modeling of CF-like features that is currently being undertaken.

Acknowledgement

This study was supported by the office of Naval Research under contracts N00014-82-0404 as part of the High Energetic Benthic Boundary Layer Experiment (HEBBLE) program and N00014-87G-011S. One of us (TE) was

partially supported by the Oceanographic and Limnological Research Institute of Israel. We are grateful to J. Deardorff for reviewing an earlier version of this paper. We thank P. Klein for her assistance with the manuscript.

References

Adams, C. E., Jr., and G. L., Weatherly: 1981, 'Some Effects of Suspended Sediment Stratification on an Oceanic Bottom Boundary Layer', *J. Geophys. Res.* **86**, 4161–4172.

Amos, A. F., Gordon, A. L., and Schneider, E. D.: 1971, 'Water Masses and Circulation Patterns in the Regions of the Blake-Bahama Outer Ridge', *Deep-Sea Res.* **18**, 145–165.

Arya, S. P. S.: 1973, 'Neutral Planetary Boundary Layer above a Nonhomogeneous Surface', *Geophys. Fluid Dyn.* **4**, 333–355.

Brost, R. A. and Wyngaard, J. C.: 1978, 'A Model Study of the Stably Stratified Planetary Boundary Layer', *J. Atmos. Sci.* **35**, 1427–1440.

Businger, J. A. and Arya, S. P. S.: 1974, 'Height of the Mixed Layer in the Stably Stratified Planetary Boundary Layer, Advances in Geophysics', *Adv. Geophys.* **18A**, Academic Press, pp. 407–418.

Deardorff, J. W.: 1970, 'A Three Dimensional Numerical Investigation of the Idealized Planetary Boundary Layer', *Geophys. Fluid Dyn.* **1**, 377–410.

Ebbesmeyer, C. C., Taft, B. A., McWilliams, J. C., Shen, C. Y., Riser, S. C., and Rossby, H. T.: 1986, 'Detection, Structure, and Origin of Extreme Anomalies in a Western Atlantic Oceanographic Section', *J. Phys. Oceanogr.* **16**, 591–612.

Ezer, T. and Weatherly, G. L.: 1989, 'Small-scale Spatial Structure and Long-term Variability of near Bottom Layers in the HEBBLE Area', to appear in *Deep-Sea Res.*

Gross, T. F., Williams, A. J., and Grant, W. D.: 1986, 'Long Term in-situ Calculations of Kinetic Energy and Reynolds Stress in a Deep Sea Boundary Layer', *J. Geophys. Res.* **91**, 8461–8469.

Gryning, S. E., Ulden, A. P., and Larsen, S. E.: 1983, 'Dispersion from a Continuous Ground-Level Source Investigated by a *K* Model', *Quart. J. R. Meteorol. Soc.* **109**, 355–364.

Lettau, H. H. and Dabberdt, W. F.: 1970, 'Variangular Wind Spirals', *Boundary-Layer Meteorol.* **1**, 64–79.

Long, C. E.: 1981, *A Simple Model for Time-Dependent Stably Stratified Turbulent Boundary Layer*, Ref. M 81-04, Dept. of Oceanography, University of Washington.

McLean, S. R. and Yean, J.: 1987, 'Velocity and Stress in the Deep-ocean Boundary Layer', *J. Phy. Oceanogr.* **17**, 1356–1365.

Mellor, G. L. and Yamada, T.: 1974, 'A Hierarchical Structure and Long-term Variability of Near Bottom Layers', *J. Atmos. Sci.* **31**, 1791–1806.

Mofjeld, H. O. and Lavelle, J. W.: 1984, 'Setting the Length Scale in a Second Order Closure Model of the Unstratified Bottom Boundary Layer', *J. Phys. Oceanogr.* **14**, 833–839.

Nof, D.: 1983, 'The Translation of Isolated Cold Eddies on a Sloping Bottom', *Deep-Sea Res.* **30**, 171–182.

Nof, D.: 1984, 'Oscillatory Drift of Deep Cold Eddies', *Deep-Sea Res.* **31**, 1359–1414.

O'Brien, J. J.: 1970, 'A Note on the Vertical Structure of the Eddy Exchange Coefficient in the Planetary Boundary Layer', *J. Atmos. Sci.* **27**, 1213–1215.

Richards, K. J.: 1982, 'Modeling the Benthic Boundary Layer', *J. Phys. Oceanogr.* **12**, 428–439.

Smith, P. C.: 1975, 'A Streamtube Model for Bottom Boundary Current in the Ocean', *Deep Sea Res.* **22**, 853–873.

Tennekes, H. and Lumley, J. J.: 1972, *A First Course in Turbulence*, MIT Press, 300 pp.

Weatherly, G. L.: 1975, 'A Numerical Study of Time-dependent Turbulent Ekman Layers over Horizontal and Sloping Bottoms', *J. Phys. Oceanogr.* **5**, 288–299.

Weatherly, G. L. and Martin, P. J.: 1978, 'On the Structure and Dynamics of the Oceanic Bottom Boundary Layer', *J. Phys. Oceanogr.* **8**, 557–570.

Weatherly, G. L. and Kelley, E. A.: 1982, '"Too Cold" Bottom Layers at the Base of the Scotial Rise', *J. Mar. Res.* **40**, 985–1012.

Weatherly, G. L. and Kelley, E. A.: 1985, 'Two Views of the Cold Filament', *J. Phys. Oceanogr.* **15**, 68–81.